

---

## X-Ray Structural Studies of Rubisco from *Rhodospirillum rubrum* and Spinach

C.-I. Branden, G. Schneider, Y. Lindqvist, I. Andersson, S. Knight and G. H. Lorimer

*Phil. Trans. R. Soc. Lond. B* 1986 **313**, 359-365

doi: 10.1098/rstb.1986.0043

---

### References

Article cited in:

<http://rstb.royalsocietypublishing.org/content/313/1162/359#related-urls>

### Email alerting service

Receive free email alerts when new articles cite this article - sign up in the box at the top right-hand corner of the article or click [here](#)

---

To subscribe to *Phil. Trans. R. Soc. Lond. B* go to: <http://rstb.royalsocietypublishing.org/subscriptions>

---

## X-ray structural studies of Rubisco from *Rhodospirillum rubrum* and spinach

BY C.-I. BRÄNDÉN<sup>1</sup>, G. SCHNEIDER<sup>1</sup>, Y. LINDQVIST<sup>1</sup>, I. ANDERSSON<sup>1</sup>, S. KNIGHT<sup>1</sup>  
AND G. H. LORIMER<sup>2</sup>

<sup>1</sup> *Department of Molecular Biology, Swedish University of Agricultural Sciences, Uppsala Biomedical Center, Box 590, S-751 24 Uppsala, Sweden.*

<sup>2</sup> *Central Research and Development Department, E. I. du Pont de Nemours and Co, Wilmington, Delaware 19898, U.S.A.*

[Plate 1]

An electron density map to 2.9 Å (1 Å = 10<sup>-10</sup> m) resolution of Rubisco from *Rhodospirillum rubrum* has been obtained from crystals of the gene product expressed in *Escherichia coli*. These crystals are monoclinic, space group  $P2_1$  with cell dimensions  $a = 65.5$  Å,  $b = 70.6$  Å,  $c = 104.1$  Å and  $\beta = 92^\circ$  and with two subunits per asymmetric unit. Isomorphous phases were obtained from three heavy atom derivatives. The dimeric molecule has the shape of a distorted ellipsoid with approximate dimensions 45 × 70 × 105 Å. The subunit interactions in the dimeric molecule are tight and extensive. Each subunit is divided into two main domains, one of which has extensive  $\alpha/\beta$  structure probably folded into the common eight unit barrel structure. NADPH and pyridoxal phosphate bind at one end of this domain in each subunit.

Two different octameric molecules with approximate (422) symmetry have been constructed from the L<sub>2</sub> dimeric molecule from *R. rubrum*, assuming that the molecular twofold axis of the L<sub>2</sub> dimer is preserved in the L<sub>8</sub> molecule. It is shown that only one of these is compatible with the orthorhombic crystal lattice of spinach and *Alcatigenes eutrophus* Rubisco. The L<sub>8</sub> molecule thus obtained is ellipsoidal with approximate dimensions 130 Å × 130 Å × 105 Å and with a large hole in the middle of about 40 Å diameter around the fourfold axis. A cleft in each subunit between the two domains could form a binding site for the small subunit in the plant L<sub>8</sub>S<sub>8</sub> Rubisco molecule.

### 1. RHODOSPIRILLUM RUBRUM RUBISCO

#### (a) Introduction

Rubisco from the photosynthetic bacterium *Rhodospirillum rubrum* is a dimeric molecule of 56-kDa subunits which catalyses both the carboxylase and the oxygenase reaction. The enzyme was first crystallized by Schloss *et al.* (1979). Subsequently the gene was cloned (Somerville & Somerville 1984) and sequenced (Nargang *et al.* 1984). The sequence was found to have about 33% identity to the large subunit of any plant enzyme with a much higher identity in the active site peptides. Three different groups (Schneider *et al.* 1984; Janson *et al.* 1984; Choe *et al.* 1985) have reported a similar tetragonal crystal form from either the native enzyme or the cloned gene product, which contains an additional 24 amino acids from  $\beta$ -galactosidase. These crystals are tetragonal, space group  $P4_12_12$  or  $P4_32_12$ , with cell dimensions  $a = b = 82$  Å† and  $c = 290$  Å or 324 Å.

† 1 Å = 10<sup>-10</sup> m = 10<sup>-1</sup> nm.

[ 55 ]

Due to the rather long  $c$ -axis and poor diffraction quality of these crystals we started to search for better crystal forms of this enzyme from the cloned gene product. We have obtained two new crystal forms, one monoclinic and one orthorhombic (Schneider *et al.* 1986). The monoclinic crystals diffract to at least 1.9 Å resolution (figure 1c) and all work reported here has been obtained from this crystal form.

(b) *X-ray work*

The monoclinic crystals belong to space group  $P2_1$  with cell dimensions  $a = 65.5$  Å,  $b = 70.6$  Å,  $c = 104.1$  Å and  $\beta = 92.1^\circ$ . The asymmetric unit contains one dimeric molecule. All X-ray data have been collected at 4 °C on a STOE four circle diffractometer equipped with a graphite monochromator.

About 50 heavy metal compounds were tested to obtain heavy atom derivatives. Ten of these gave reproducible intensity differences, and low resolution data sets were collected for all of them. Three of these data sets were useful for phase-determination. These heavy atom derivatives were obtained by soaking native crystals for six days against 7 mM  $\text{KAu}(\text{CN})_2$ , ten days against 5 mM ethylmercurithiosalicylate and one week against 1 mM  $\text{SmCl}_3$ .

X-ray data were collected to 2.9 Å resolution for native crystals and for two of the derivatives. For the third derivative,  $\text{SmCl}_3$ , data were collected only to 4.4 Å resolution due to bad phasing power at higher resolution.

The heavy atom positions were determined from difference Patterson and Fourier maps. We found six gold, two mercury and four samarium positions. The parameters for all sites were refined by the method of least squares, with the use of phase angles obtained from all three derivatives. The final figure of merit to 2.9 Å was 0.43.

Rotation function calculations using native data indicated the presence of a local twofold rotation axis perpendicular to the monoclinic axis. The parameters defining this axis were refined from the observed heavy atom positions. The root mean square deviation between equivalent heavy atom positions was 0.7 Å.

Before calculation of the final electron density map, the phase angles were improved by a solvent flattening procedure (with B. C. Wang's program system). The resulting electron density map shows the molecular and subunit boundaries and the domain organization of the subunits as well as a number of secondary structure elements, but does not allow unambiguous tracing of the chain. We are at present improving the phase angles by using Bricogne's non-crystallographic symmetry averaging procedure.

(c) *Description of the molecule*

The dimeric molecule has the shape of a distorted ellipsoid with dimensions 45 Å × 70 Å × 105 Å, where the 45 Å principal axis of the ellipsoid is the twofold molecular axis. Each subunit is very clearly organized in two main domains, A and B. Figure 2a, b shows two schematic views of the molecule perpendicular to the long axis. Figure 2c shows a schematic cross-section of the molecule in the plane of the twofold axis perpendicular to the long axis of the molecule.

Domain A has an extensive  $\alpha/\beta$  structure. Eight helices can be identified; these have a similar relative arrangement to the eight helices of the common  $\alpha/\beta$ -barrel motif that has been found in a number of enzymes including triose phosphate isomerase (Banner *et al.* 1975) and glycollate oxidase (Lindqvist & Brändén 1975). Domain B contains a few helices and some antiparallel

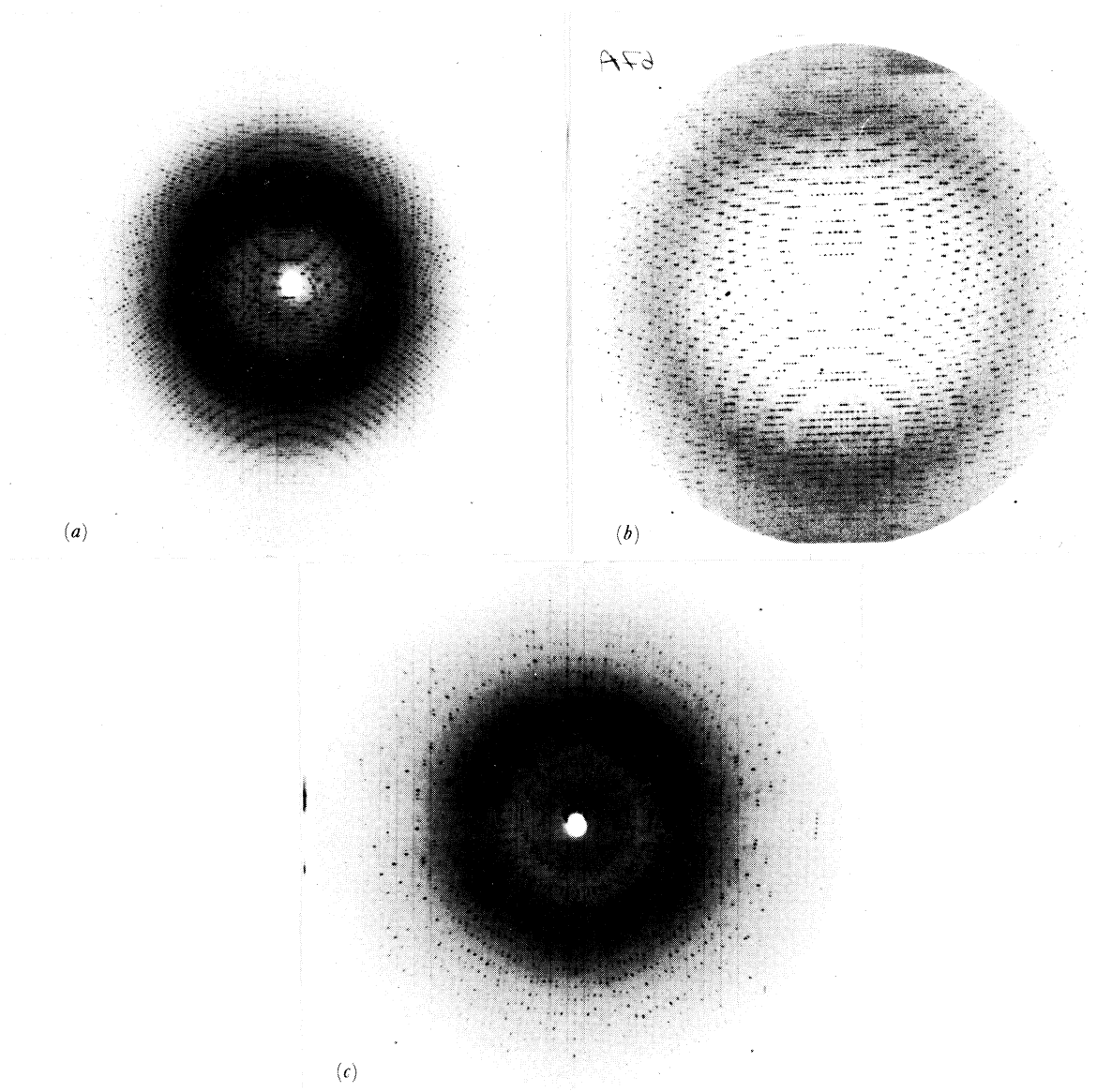


FIGURE 1. Diffraction patterns of Rubisco crystals from *R. rubrum* and spinach: (a) Spinach Rubisco. 1.4 Å resolution, 0.5° oscillation. Photograph taken at the Daresbury wiggler beam line with a wave-length of 0.86 Å. (b) Spinach Co-substituted Rubisco. 2.4 Å resolution, 1° oscillation; Daresbury wiggler beam line. (c) *R. rubrum* Rubisco. 1.9 Å resolution, 1° oscillation. Photograph taken at an Elliot rotating anode.

(Facing p. 360)

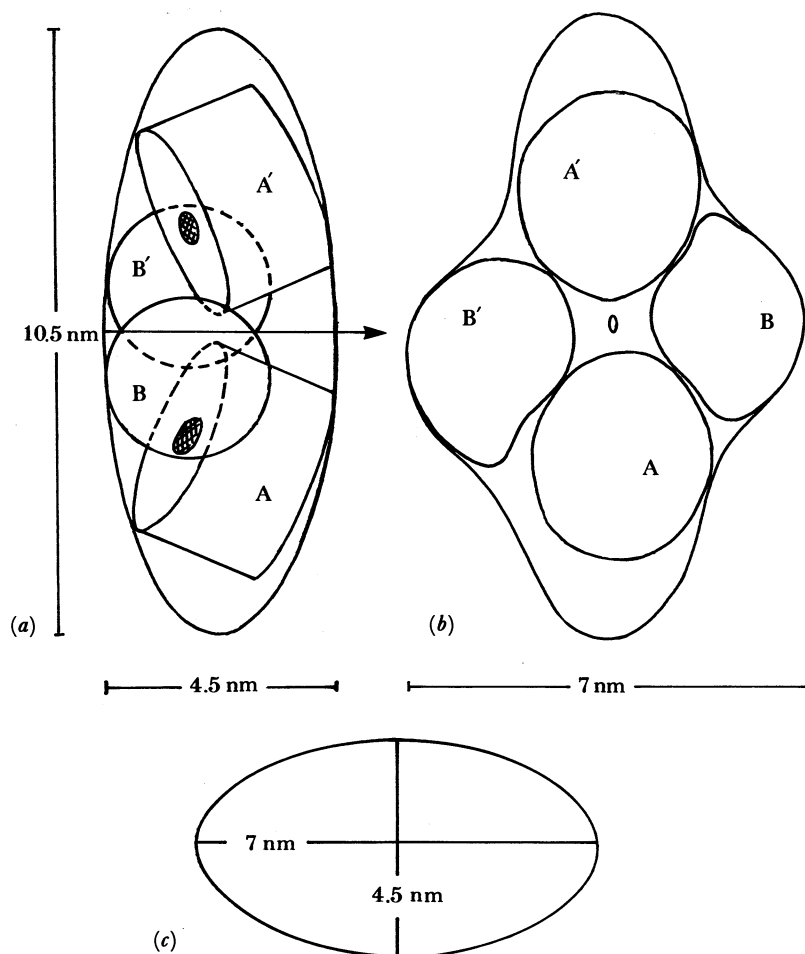


FIGURE 2. Schematic views of the *R. rubrum* molecule in three different directions. A and B are approximate outlines of the two domains of one subunit; A' and B' are in the second subunit. (a) View down the y-axis. The arrow denotes the molecular twofold axis. NADPH and pyridoxal phosphate bind in the vicinity of the hatched area. (b) View down the local twofold axis. (c) Cross-section through the middle of the molecule in a plane perpendicular to the long axis of the molecule. The local twofold axis is in this plane along the short axis of the ellipsoid.

$\beta$ - structure. We have not been able to see similarities with any other known domain motif for domain B.

Our crystals contain the non-activated form of the enzyme (Schneider *et al.* 1986). To identify the region of the active site in this crystal form, we soaked NADPH or pyridoxal phosphate into two different crystals. X-ray data were collected to 6.3 Å for these crystals, and difference Fourier maps were computed. The highest peaks in those maps, which were five times the background, were in the same region but at slightly different positions. This region is at one end of the proposed barrel structure, domain A, at a position which corresponds to one end of the strands of the barrel. Peaks were found at equivalent positions in both subunits.

In all known  $\alpha/\beta$  barrel structures, the active site is at the carboxyl end of the strands of the barrel. It thus seems rather likely that domain A is an  $\alpha/\beta$  barrel, which provides the active site of Rubisco.

## 2. SPINACH RUBISCO

(a) *Introduction*

The vast majority of photosynthetic organisms have a Rubisco molecule which is built up from eight large subunits and eight small subunits ( $L_8S_8$ ). Four groups have reported crystallographic data on the  $L_8S_8$  molecule. The group in Los Angeles has reported several crystal forms for the tobacco enzyme (Baker *et al.* 1975; Baker *et al.* 1977) and has also shown that the potato enzyme crystallizes isomorphously with form III of the tobacco enzyme (Johal *et al.* 1980). The group in Berlin studies the enzyme from the hydrogen bacterium *Alcaligenes eutrophus* (Bowien *et al.* 1980; Pal *et al.* 1985); the enzyme from spinach was first crystallized by Johal & Borque (1979). Preliminary X-ray data for the spinach enzyme have been reported from both the Oxford group (Barcena *et al.* 1983) and our group in Uppsala (Andersson *et al.* 1983; Andersson & Brändén 1984).

(b) *Comparison of the  $C222_1$  crystal forms of Rubisco*

The enzyme from *Alcaligenes eutrophus* crystallizes in the same spacegroup as the spinach crystals reported from Oxford and Uppsala, and has very similar cell dimensions. These crystals are orthorhombic, space group  $C222_1$ , with cell dimensions  $a = 159 \text{ \AA}$ ,  $b = 159 \text{ \AA}$  and  $c = 201 \text{ \AA}$  and with half the  $L_8S_8$  molecule in the asymmetric unit. In spite of these similarities, the intensities of the X-ray patterns are quite different; they thus represent different crystal forms, presumably with different packing arrangements of similar molecules. Both the Berlin group and the Uppsala group have experienced problems with twinning of some crystals due to a rotation of  $90^\circ$  around the  $c$ -axis. The Oxford group has an unusual pattern of absent reflections; this pattern has been interpreted in terms of a particular packing arrangement.

The crystals we obtained diffracted extremely well, with reflections visible at  $1.4 \text{ \AA}$ . We have collected native data to  $2.4 \text{ \AA}$  resolution as well as data for three different Hg-derivatives to the same resolution. Figure 1 *a, b* (plate 1) shows two oscillation photographs of Co-substituted Rubisco recently taken at the Daresbury synchrotron source using the wiggler beam line. Low resolution X-ray data show the presence of a pseudo-fourfold axis parallel to  $c$  and also a pseudo-F-centring of the reflections. This pseudosymmetry is independent of the twinning problem, since it is not present at high resolution for untwinned crystals.

From our data and from published photographs from the other groups, we have compared some reflections that are not affected by this particular twinning. Table 1 lists ( $hh0$ ) and ( $00l$ ) reflections below  $10 \text{ \AA}$  resolution from the three crystal forms. It is apparent from this table that the large differences must reflect differences in the packing arrangement of the molecules. There are two principally different ways to pack molecules with pseudo ( $422$ ) symmetry in space group  $C222_1$ . These are illustrated in figure 3. If the molecular centre is at the origin, the screw axis along  $c$  will position another molecule with its centre at  $x = 0$ ,  $y = 0$ ,  $z = \frac{1}{2}$ . The molecules will thus pack on top of each other along  $c$ . This is the arrangement discussed by Barcena *et al.* (1983) for the Oxford crystal form. At low resolution one would expect this arrangement to give rise to a pseudocell with half the length of the  $c$ -axis.

The second possibility is illustrated in figure 3 *b*. Here the molecular centre is at  $x = \frac{1}{4}$ ,  $y = 0$ ,  $z = 0$  (or  $x = 0$ ,  $y = \frac{1}{4}$ ,  $z = 0$ ). The screw axis along  $c$  generates another molecule at  $x = \frac{3}{4}$ ,  $y = 0$ ,  $z = \frac{1}{2}$ . The molecular centres at  $z = 0$  and  $z = \frac{1}{2}$  are here not on top of each other but displaced by half the length of the  $a$ - or  $b$ -axis. The packing within each layer is the same, but

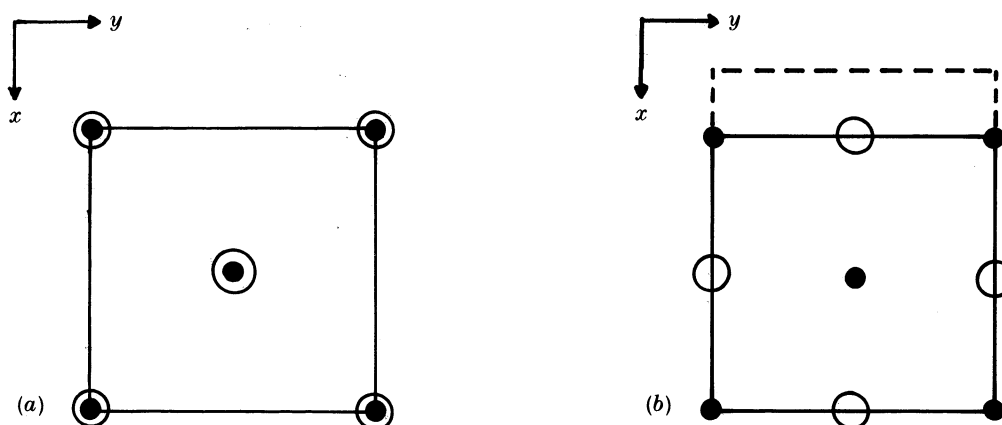


FIGURE 3. Possible packing arrangement of Rubisco molecules with pseudo  $(422)$  symmetry in space group  $C222_1$ . Small solid circles represent molecules with centre at  $z = 0$ ; large open circles have their centres at  $z = \frac{1}{2}$ . (a) Molecular centre at  $x = 0, y = 0$ . (b) Molecular centre at  $x = \frac{1}{4}, y = 0$ .

TABLE 1. COMPARISON OF SOME LOW RESOLUTION REFLECTIONS THAT ARE NOT AFFECTED BY POSSIBLE TWINNING

$(hkl)$	Uppsala	Berlin	Oxford
(006)	—	vs	—
(008)	vs	vs	vs
(0010)	m	vw	s
(0012)	m	s	m
(0014)	w	—	—
(0016)	—	—	s
(0018)	vs	—	vs
(0020)	m	—	m
(440)	w	vs	—
(550)	—	—	—
(660)	m	s	—
(770)	—	—	—
(880)	w	s	—
(990)	vw	vw	—
(10100)	vs	vs	vs
(11110)	—	—	—
(12120)	vw	vw	—

Abbreviations: vs, very strong; s, strong; m, medium; w, weak; vw, very weak; —, absent.

the layers at  $z = 0$  and  $z = \frac{1}{2}$  are displaced relative to each other. This arrangement gives rise to pseudo-F-centring at low resolution, just what we observe for our crystals. We have thus concluded that this is the packing arrangement for our crystal form.

(c) *A possible model for the  $L_8S_8$  molecule*

We have observed that the subunit interactions are tight and extensive in the  $L_2$  dimer of the *R. rubrum* enzyme. If we assume that this interaction is preserved in the  $L_8S_8$  molecule, we can construct a model of the  $L_8$  part of this molecule based on four  $L_2$  dimers around a fourfold axis. There are in principle two different such octameric molecules that could be packed into the  $C222_1$  lattice. These are illustrated in figures 4 and 5 respectively. The ellipses in these figures correspond to the cross-section (figure 2c) through the middle of the molecule. The

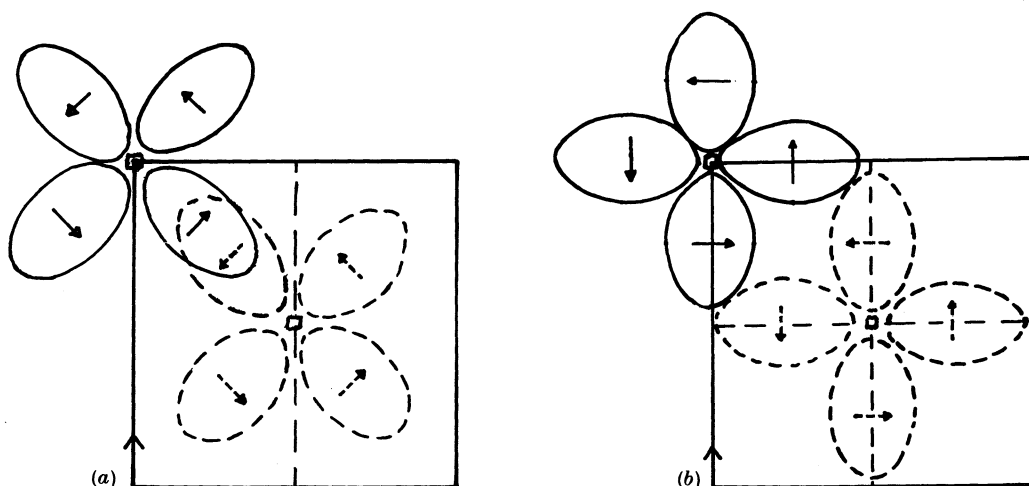


FIGURE 4. Arrangement of  $L_2$  dimers into an  $L_8$  molecule in a cloverleaf fashion: (a) The crystallographic twofold axis along  $a$  passes between two dimers. (b) The crystallographic twofold axis along  $a$  passes through two dimers.

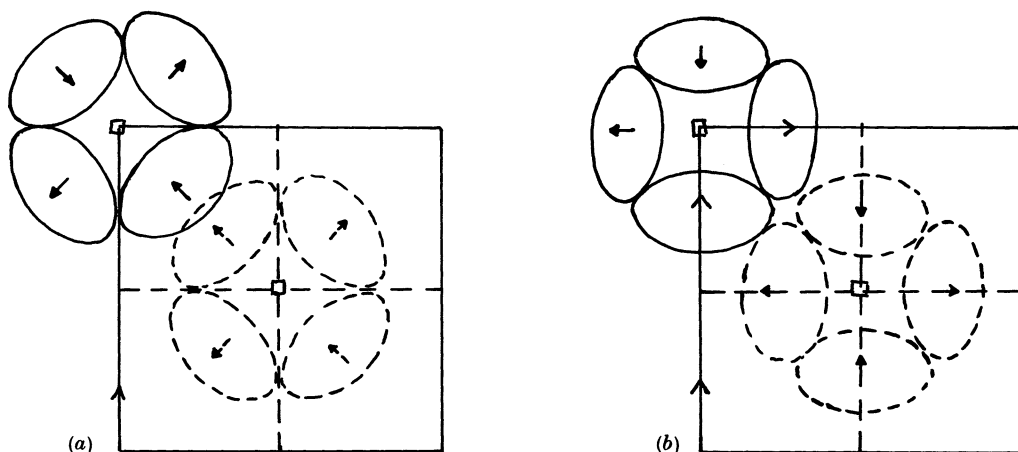


FIGURE 5. Arrangement of  $L_2$  dimers into an  $L_8$  molecule in a blockhouse fashion: (a) The crystallographic twofold axis along  $a$  passes between two dimers. (b) The crystallographic twofold axis along  $a$  passes through two dimers.

dimensions of this ellipse are drawn to the same scale as the unit cell of the  $C222_1$  crystals. The arrangement in figure 4b is immediately ruled out, since the crystallographic twofold axis along  $a$  would correspond to a non-existent twofold axis through the molecule. The arrangement in figure 4a is compatible with the crystallographic symmetry for one molecule but is incompatible with packing requirements. On the other hand, both arrangements in figure 5 are possible both from symmetry and packing requirements.

We can thus build an approximate model of the  $L_8$  molecule (figure 5). The dimensions of this  $L_8$  molecule would be approximately  $130 \text{ \AA} \times 130 \text{ \AA} \times 105 \text{ \AA}$ . There would be a large hole in the middle, around the fourfold axis, of about  $40 \text{ \AA}$  diameter. The active sites as located in the  $L_2$  dimer would be on the outside of the molecule. There is a cleft in each subunit between the two domains. If the small subunit binds in this cleft we would obtain a model of the  $L_8S_8$  molecule which to a first gross approximation is similar to the one proposed by Bowien *et al.* (1980) on the basis of electron microscopy.



## REFERENCES

- Andersson, I., Tjäder, A.-C., Cedergren-Zeppezauer, R. & Brändén, C.-I. 1983 Crystallization and preliminary X-ray studies of spinach Ribulose-1,5-bisphosphate carboxylase/oxygenase complexed with activator and a transition state analogue. *J. biol. Chem.* **258**, 14088–14090.
- Andersson, I. & Brändén, C.-I. 1984 Large single crystals of spinach Ribulose-1,5-bisphosphate carboxylase/oxygenase suitable for X-ray studies. *J. molec. Biol.* **172**, 363–366.
- Baker, T. S., Suh, S. W. & Eisenberg, D. 1977 Structure of ribulose-1,5-bisphosphate carboxylase-oxygenase: Form III crystals. *Proc. natn. Acad. Sci. U.S.A.* **74**, 1037–1041.
- Baker, T. S., Eisenberg, D., Eiserling, F. A. & Weissman, L. 1975 The structure of form I crystals of D-Ribulose-1,5-diphosphate carboxylase. *J. molec. Biol.* **91**, 391–399.
- Banner, D. W., Bloomer, H. C., Petsko, G. A., Phillips, D. C., Pogson, C. I. & Wilson, A. I. 1975 Structure of chicken muscle triose phosphate isomerase. *Nature, Lond.* **255**, 609–614.
- Barcena, J. A., Pickersgill, R. W., Adams, M. J., Phillips, D. C. & Whately, F. R. 1983 Crystallization and preliminary X-ray data of Ribulose-1, 5-bisphosphate carboxylase from spinach. *EMBO J.* **2**, 2363–2367.
- Bowien, B., Mayer, F., Spiess, E., Pähler, A., Englisch, U. & Saenger, W. 1980 On the structure of crystalline Ribulosebisphosphate carboxylase from *Alcaligenes eutrophus*. *Eur. J. Biochem.* **106**, 405–410.
- Choe, H.-W., Jakob, R., Hahn, U. & Pal, G. P. 1985 Crystallization of the activated ternary complex of Ribulose-1,5-bisphosphate carboxylase-oxygenase isolated from *Rhodospirillum rubrum* and an *Escherichia coli* clone. *J. molec. Biol.* **185**, 781–783.
- Janson, C. A., Smith, W. W., Eisenberg, D. & Hartman, F. C. 1984 Preliminary structural studies of Ribulose-1,5-bisphosphate carboxylase/oxygenase from *Rhodospirillum rubrum*. *J. biol. Chem.* **259**, 11594–11596.
- Johal, S. & Bourque, D. P. 1979 Crystalline Ribulose 1,5-bisphosphate carboxylase-oxygenase from spinach. *Science, Wash.* **204**, 75–77.
- Johal, S., Bourque, D. P., Smith, W. W., Suh, S. W. & Eisenberg, D. 1980 Crystallization and characterization of Ribulose-1,5-bisphosphate carboxylase/oxygenase from eight plant species. *J. biol. Chem.* **255**, 8873–8880.
- Lindqvist, Y. & Brändén, C.-I. 1985 Structure of glycolate oxidase from spinach. *Proc. natn. Acad. Sci. U.S.A.* **82**, 6855–6859.
- Nargang, F., McIntosh, L. & Somerville, G. 1984 Nucleotide sequence of the Ribulosebisphosphate carboxylase gene from *Rhodospirillum rubrum*. *Molec. gen. Genet.* **193**, 220–224.
- Pal, G. P., Jakob, R., Han, U., Bowien, R. & Saenger, W. 1985 Single and twinned crystals of Ribulose-1,5-bisphosphate carboxylase-oxygenase from *Alcaligenes eutrophus*. *J. biol. Chem.* **260**, 10768–10770.
- Schloss, J. V., Phares, E. F., Long, M. V., Norton, I. L., Stringer, C. D. & Hartman, F. C. 1979 Isolation, characterization and crystallization of Ribulosebisphosphate carboxylase from autotrophically grown *Rhodospirillum rubrum*. *J. Bact.* **137**, 490–501.
- Schneider, G., Brändén, C.-I. & Lorimer, G. 1984 Preliminary X-ray diffraction study of Ribulose-1,5-bisphosphate carboxylase from *Rhodospirillum rubrum*. *J. molec. Biol.* **175**, 99–102.
- Schneider, G., Brändén, C.-I. & Lorimer, G. 1986 New crystal forms of Ribulose-1,5-bisphosphate carboxylase/oxygenase from *Rhodospirillum rubrum*. *J. molec. Biol.* **187**, 141–143.
- Somerville, C. R. & Somerville, S. C. 1984 Cloning and expression of the *Rhodospirillum rubrum* Ribulosebisphosphate carboxylase gene in *E. coli*. *Molec. gen. Genet.* **193**, 214–219.

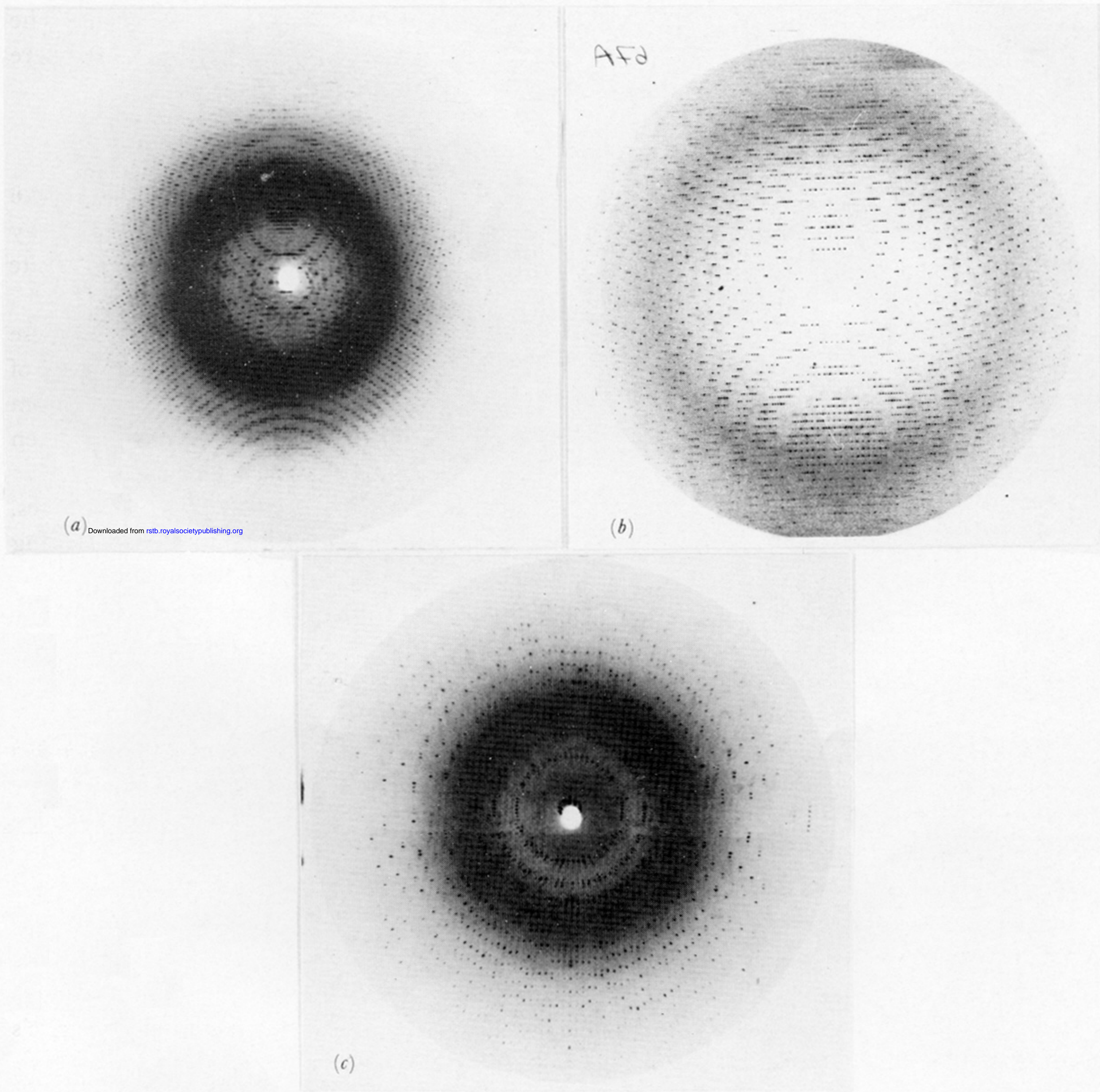


FIGURE 1. Diffraction patterns of Rubisco crystals from *R. rubrum* and spinach: (a) Spinach Rubisco. 1.4 Å resolution, 0.5° oscillation. Photograph taken at the Daresbury wiggler beam line with a wave-length of 0.86 Å. (b) Spinach Co-substituted Rubisco. 2.4 Å resolution, 1° oscillation; Daresbury wiggler beam line. (c) *R. rubrum* Rubisco. 1.9 Å resolution, 1° oscillation. Photograph taken at an Elliot rotating anode.